

Gaussian process test for high-throughput sequencing time series: application to experimental evolution

Hande Topa¹, Ágnes Jónás^{2,3}, Robert Kofler²,
Carolyn Kosiol² and Antti Honkela⁴

¹ Helsinki Institute for Information Technology HIIT, Department of
Information and Computer Science, Aalto University, Espoo, Finland

² Institut für Populationsgenetik, Vetmeduni Vienna, Wien, Austria

³ Vienna Graduate School of Population Genetics, Wien, Austria

⁴ Helsinki Institute for Information Technology HIIT, Department of
Computer Science, University of Helsinki, Helsinki, Finland

Abstract

Motivation: Recent advances in high-throughput sequencing (HTS) have made it possible to monitor genomes in great detail. New experiments not only use HTS to measure genomic features at one time point but to monitor them changing over time with the aim of identifying significant changes in their abundance. In population genetics, for example, allele frequencies are monitored over time to detect significant frequency changes that indicate selection pressures. Previous attempts at analysing data from HTS experiments have been limited as they could not simultaneously include data at intermediate time points, replicate experiments and sources of uncertainty specific to HTS such as sequencing depth.

Results: We present the beta-binomial Gaussian process (BBGP) model for ranking features with significant non-random variation in abundance over time. The features are assumed to represent proportions, such as proportion of an alternative allele in a population. We use the beta-binomial model to capture the uncertainty arising from finite sequencing depth and combine with a Gaussian process model over the time series. In simulations that mimic the features of experimental evolution data, the proposed method clearly outperforms classical testing in average precision of finding selected alleles. We also present results on real data from *Drosophila* experimental evolution experiment in temperature adaptation.

Availability: R software implementing the test is available at <https://github.com/handetopa/BBGP>.

1 Introduction

Most biological processes are dynamic and analysis of time series data is necessary to understand them. Recent advances in high-throughput sequencing (HTS) technologies have provided new experimental approaches to collect genome-wide time series. For example, experimental evolution now uses a new evolve and re-sequencing (ER) approach to understand which genes are targeted by selection and how (Burke and Long, 2012, Kawecki *et al.*, 2012). Such experiments enable phenotypic divergence to be forced in response to changes in only few environmental conditions in the laboratory while other conditions are kept constant. The evolved populations are then subjected to HTS.

Experimental evolution in microorganisms has focused on the fate new mutations. For example, in *Escherichia coli* bacteria (Barrick *et al.*, 2009) and *Saccharomyces cerevisiae* (Lang *et al.*, 2013) new mutations were studied and their effect in large populations was modelled (e.g., Illingworth *et al.*, 2012). In contrast, ER experiments with sexually reproducing multicellular organisms address selection on standing variation and allele frequency changes (AFCs) in small populations where drift plays an important role. For example, for *Drosophila melanogaster* (*Dmel*), several phenotypic traits, such as accelerated development (Burke *et al.*, 2010), body size variation (Turner *et al.*, 2011), hypoxia-tolerance (Zhou *et al.*, 2011) and temperature adaptation (Orozco-TerWengel *et al.*, 2012) have been investigated. Motivated by these experimental studies, we believe that experimental evolution combined with HTS supplies a good basis for studying AFC through time series molecular data.

To perform allele frequency comparisons, pairwise statistical tests between base and evolved populations were typically carried out. Burke *et al.* (2010) combined Fisher’s exact tests with a sliding-window approach to identify genomic regions that show allele frequency differences between populations selected for accelerated development and controls without direct selection. Turner *et al.* (2011) developed a pairwise summary statistic, called ”diff-Stat” to estimate the observed distribution of allele frequency differences and compared this to the expected distribution without selection. Orozco-TerWengel *et al.* (2012) identify SNPs with a consistent AFC among replicates by performing a Cochran-Mantel-Haenszel test (CMH) (Agresti, 2002). The latter is an extension of the Fisher’s exact test to multiple replicates. All above-mentioned statistical methods are based on pairwise comparisons between the base and evolved populations and do not take full advantage of the time series data now available. Here, we propose an alternative Gaussian process (GP) based approach to study AFCs over the entire time series experiment.

GP is a non-parametric statistical model that is extremely well-suited for modelling HTS time series data which usually have relatively few time points that may be irregularly sampled. Recently, there have been some works applying GP models with parameters describing the process of evolution (e.g., Jones and Moriarty, 2013 account for phylogenetic relationships, Palacios and Minin, 2013 for effective population size). GPs have also recently been applied to gene expression time series by a number of authors (Yuan, 2006; Gao *et al.*, 2008; Kirk and Stumpf, 2009; Liu *et al.*, 2010; Honkela *et al.*, 2010; Stegle *et al.*, 2010; Cooke *et al.*, 2011; Kalaitzis and Lawrence, 2011; Titsias *et al.*, 2012; Liu and Niranjana, 2012; Äijö *et al.*, 2013; Hensman *et al.*, 2013). In differential analysis, GPs have been applied to detect differences in gene expression time series in a two-sample setting by Stegle *et al.* (2010) and for detecting significant changes by Kalaitzis and Lawrence (2011). While these methods provide a very sensible basis for detecting the changing alleles, they fail to properly take into account all aspects of the available HTS data, such as differences in sequencing depth between different alleles and time points. These differences can have a huge impact in the reliability of different measured allele frequencies and taking them into account is vital for achieving good accuracy with the available short time series.

2 Methods

To identify the candidate alleles which evolve under selection, we model the allele frequencies by Gaussian Process (GP) regression. We fit time-dependent and time-independent GP models and rank the alleles according to their corresponding Bayes factors, i.e. the ratio of the marginal likelihoods under the different models.

GPs provide a convenient approach for modelling short time series. However, when applying them to a large number of short parallel time series as in many genomic applications, naive application leads to overfitting or underfitting in some examples. While these problems are rare, the bad examples can easily dominate the ranking. We overcome these challenges by excluding nonsensical parameter values, for example using a good variance model that can be incorporated into the GP models.

2.1 Data and Preprocessing

In the following, we use the term SNP for the markers and alleles under study, but the methods can be applied to any features whose abundance can be quantified in a similar manner. We assume that the SNPs are bi-allelic for a specific position of the genome in a population. In other words, only two of the alleles from (A, T, C, G) can be observed at each SNP position. We first determine the abundances of these two specific alleles and we aim to model the time dependency of the rising allele's frequency over several generations. We will refer to generations as time points for simplicity.

We denote the replicate index of each observation by r_j and the time point by t_j , $j = 1, \dots, J$, with J denoting the total number of observations. For each of these points, we assume HTS reads have been aligned to a reference genome with y_{ij} reads with a specific allele at SNP position i . We use n_{ij} to denote the total sequencing depth at the position.

2.2 Mean and Variance Inference: Beta-Binomial Model

We model y_{ij} as a draw from a binomial distribution with parameters n_{ij} and p_{ij} :

$$y_{ij}|n_{ij}, p_{ij} \sim \text{Bin}(n_{ij}, p_{ij}), \quad (1)$$

where p_{ij} denotes frequency of the specific allele in the population. We set a uniform Beta(1,1) prior on p_{ij} :

$$p_{ij}|\alpha, \beta \sim \text{Beta}(\alpha, \beta), \quad (2)$$

where $\alpha = 1$, $\beta = 1$.

Since beta prior is conjugate to the binomial likelihood, the posterior distribution will also be a beta distribution:

$$p_{ij}|y_{ij}, n_{ij}, \alpha, \beta \sim \text{Beta}(\alpha_{ij}^*, \beta_{ij}^*), \quad (3)$$

where

$$\begin{aligned} \alpha_{ij}^* &= \alpha + y_{ij}, \\ \beta_{ij}^* &= \beta + n_{ij} - y_{ij}. \end{aligned}$$

Then, the posterior mean and variance of p_{ij} can be calculated as:

$$\text{E}(p_{ij}|y_{ij}, n_{ij}, \alpha, \beta) = \frac{\alpha_{ij}^*}{\alpha_{ij}^* + \beta_{ij}^*} = \frac{\alpha + y_{ij}}{\alpha + \beta + n_{ij}} \quad (4)$$

$$\begin{aligned} \text{Var}(p_{ij}|y_{ij}, n_{ij}, \alpha, \beta) &= \frac{\alpha_{ij}^* \beta_{ij}^*}{(\alpha_{ij}^* + \beta_{ij}^*)^2 (\alpha_{ij}^* + \beta_{ij}^* + 1)} \\ &= \frac{(\alpha + y_{ij})(\beta + n_{ij} - y_{ij})}{(\alpha + \beta + n_{ij})^2 (\alpha + \beta + n_{ij} + 1)}. \end{aligned} \quad (5)$$

The inferred posterior means and posterior variances are used to fit the GP models as described in the following sections. As the results will show, this step is very important for incorporating the available uncertainty information into the GP models by taking into account different sequencing depths. For example, beta-binomial model assigns larger variances to the alleles with lower sequencing depths (Figure 1). Moreover, the Beta(1,1) prior on p_{ij} leads to a symmetry in the posterior mean and variance. The result of our method is therefore unaffected whichever allele is chosen.

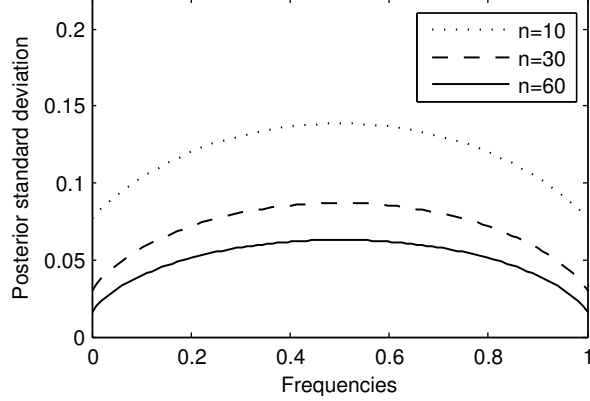


Figure 1: Posterior standard deviations of the allele frequencies with sequencing depths 10, 30, and 60.

2.3 Gaussian Process Regression

A **Gaussian process (GP)** is a collection of random variables, any finite number of which have a joint Gaussian distribution (Rasmussen and Williams, 2006). We write

$$f(t) \sim \mathcal{GP}(m(t), K(t, t')) \quad (6)$$

to denote that $f(t)$ follows a Gaussian process with mean function $m(t) = \mathbb{E}[f(t)]$ and covariance function $K(t, t') = \mathbb{E}[(f(t) - m(t))(f(t') - m(t'))]$. We let $\mathbf{y} = (y_i)_{i=1}^N$ be a vector of the noisy observations with

$$y_i = f(t_i) + \epsilon, \quad (7)$$

where ϵ is Gaussian observation noise with zero mean and a diagonal covariance matrix Σ_ϵ . To simplify the algebra we assume the mean function $m(t) = 0$ and subtract the mean of \mathbf{y} .

Gaussian processes allow marginalising the latent function to obtain a marginal likelihood. The covariance function K and the noise covariance Σ_ϵ depend on hyperparameters and parameters θ that can be estimated by maximising the log marginal likelihood:

$$\log(p(\mathbf{y}|t, \theta)) = -\frac{1}{2}\mathbf{y}^T[K(t, t) + \Sigma_\epsilon]^{-1}\mathbf{y} - \frac{1}{2}\log|K(t, t) + \Sigma_\epsilon| - \frac{n}{2}\log(2\pi). \quad (8)$$

It is also possible to compute the posterior mean and covariance at non-sampled time points t_* , given the noisy observations \mathbf{y} at sampled time points t . This is often useful for visualisation purposes. We obtain (Rasmussen and Williams, 2006):

$$f_*|y \sim \mathcal{N}(m_*, \Sigma_*), \quad (9)$$

where

$$\begin{aligned} m_* &= \mathbb{E}[f_*|\mathbf{y}] = K(t_*, t)[K(t, t) + \Sigma_\epsilon]^{-1}\mathbf{y}, \\ \Sigma_* &= K(t_*, t_*) - K(t_*, t)^T[K(t, t) + \Sigma_\epsilon]^{-1}K(t, t_*). \end{aligned}$$

In our GP models we use the squared exponential covariance matrix to model the underlying smooth function. The squared exponential covariance

$$K_{SE}(t, t') = \sigma_f^2 e^{-\frac{(t-t')^2}{2l^2}} \quad (10)$$

has two parameters: the length scale, l , and the signal variance, σ_f^2 . Length scale specifies the distance beyond which any two inputs become uncorrelated. A small length scale means that the function fluctuates very quickly, whereas a large length scale means that the function behaves like a constant function (Kalaitzis and Lawrence, 2011). Three example realisations generated with squared exponential covariance matrix can be seen in Figure 2 (a).

In the standard GP model the observation noise is assumed to be white: the noise at different time points is independent and identically distributed. The corresponding covariance matrix

$$\Sigma_\epsilon = \Sigma_W = \sigma_n^2 I \quad (11)$$

is an identity matrix multiplied by the noise variance parameter, σ_n^2 . Three example realisations generated with white noise covariance matrix can be seen in Figure 2 (b).

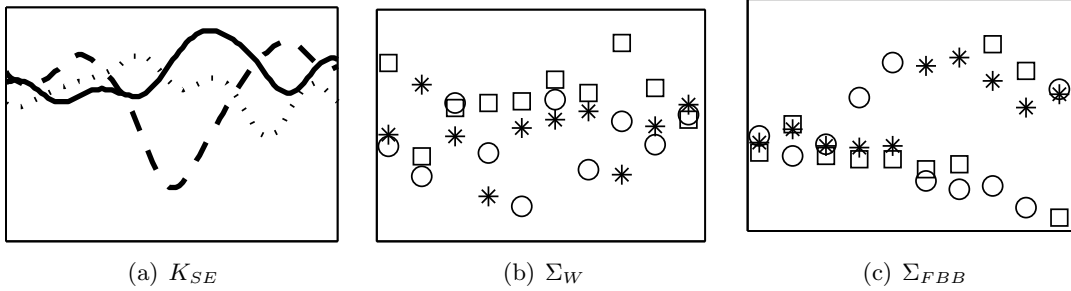


Figure 2: Example realisations from GPs and noise processes with different covariance structures.

2.4 BBGP: Beta-Binomial Gaussian Process

The Beta-Binomial Gaussian Process (BBGP) method combines beta-binomial model with the GP model in the sense that the posterior means and posterior variances of the frequencies, which are inferred by beta-binomial model, are used to fit the GP model using an additional noise covariance matrix which we call fixed beta-binomial (FBB) covariance matrix.

Returning Sec. 2.2, let us denote the posterior mean and variance of p_{ij} by m_{ij} and s_{ij}^2 , respectively. That is,

$$m_{ij} = \mathbb{E}(p_{ij}|y_{ij}, n_{ij}, \alpha, \beta) \quad (12)$$

$$s_{ij}^2 = \text{Var}(p_{ij}|y_{ij}, n_{ij}, \alpha, \beta). \quad (13)$$

To fit the BBPG model, we assume

$$m_{ij} = f(t_j) + \mu_{m_i} + \epsilon, \quad (14)$$

where $f(t) \sim \mathcal{GP}(0, K_{SE}(t, t'))$ and $\epsilon \sim N(0, \Sigma_W + \Sigma_{FBB})$. The mean μ_{m_i} is eliminated by subtracting the mean from m_{ij} . The additional covariance

$$\Sigma_{FBB} = \text{diag}(s_{ij}^2) \quad (15)$$

is a diagonal fixed beta-binomial (FBB) covariance matrix which is used to include known variance information for each observation in the GP model. The elements of Σ_{FBB} are determined by the frequency variance vector which is inferred from beta-binomial model in Sec. 2.2. Three example realisations generated with fixed beta-binomial covariance matrix can be seen in Figure 2 (c), where larger variance values were inferred for the later time points.

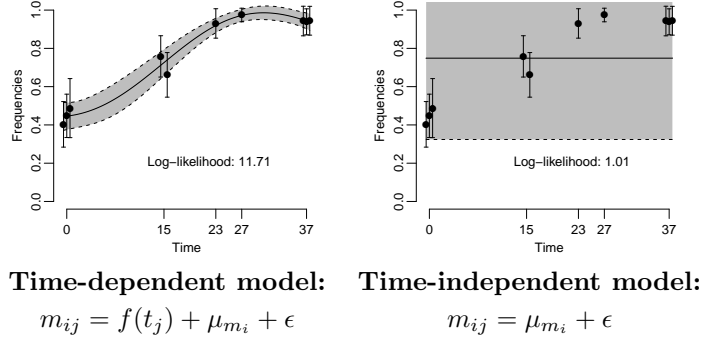


Figure 3: BBGP fits for the time-dependent and time-independent models for an example SNP taken from the real data set (Orozco-TerWengel *et al.*, 2012). Confidence regions are shown for ± 2 standard deviation. Similarly, error bars indicate ± 2 standard deviation (from FBB) interval. Replicates at the same time points are shifted by 0.5 for better visualisation.

2.5 BBGP-based test

We fit the “time-dependent” BBGP model of Eq. (14) and a “time-independent” model without the GP term $f(t_j)$ for each SNP. Thereby the parameters of the squared exponential covariance (K_{SE} , Eq. 10) in the time-dependent model and the white noise covariance (Σ_W , Eq. 11) in both models are fitted by maximising the marginal likelihood. The fixed beta-binomial covariance (Σ_{FBB} , Eq. 15) does not contain any free hyperparameters. If the model is actually time-independent, the length scale in the squared exponential covariance is estimated to be very large, which makes the maximum likelihood of the time-dependent model equivalent to that of time-independent model. Figure 3 shows an example of the time-dependent (left) and time-independent (right) BBGP models.

We maximise the log marginal likelihood functions for the models by scaled conjugate gradient method using the “gptk” package by Kalaitzis and Lawrence (2011). We use a grid search over the parameter space and initialise the parameters to the grid value with highest likelihood. We set a lower bound equal to the shortest spacing between observations for the length scale parameter to avoid overfitting.

We compute the Bayes factor (BF) for SNP i as (Stegle *et al.*, 2010; Kalaitzis and Lawrence, 2011):

$$\text{BF}_i = \frac{p(\mathbf{m}_i | \theta_1, \text{“time-dependent model”})}{p(\mathbf{m}_i | \theta_2, \text{“time-independent model”})}, \quad (16)$$

where θ_1 and θ_2 contain the maximum likelihood estimates of the hyperparameters in the corresponding BBGP models. Bayes factors indicate the degree of the models to be “time-dependent” rather than “time-independent”.

2.6 Cochran-Mantel-Haenszel Test

We compare BBPG against the Cochran-Mantel-Haenszel test (CMH), which was used by Orozco-TerWengel *et al.* (2012) to identify alleles with consistent allele frequency change across replicates. The CMH test has been proven to be the best-performing test statistic applied on HTS evolutionary data so far (Kofler and Schlötterer, 2014). Therefore, we take it as the basis of comparison with BBGP. CMH allows to test whether the joint odds ratio of replicated ($r = 1, \dots, R$) allele counts in a $2 \times 2 \times R$ contingency table (Table 1) is significantly different from one. Significant deviation from one implies dependence of allele counts between two time points that is consistent among replicates. The CMH tests pairwise observations of the two alternative allele counts $y_{ij}^{(1)}$ and $y_{ij}^{(2)}$. In our bi-allelic case $y_{ij}^{(1)} = y_{ij}$ and $y_{ij}^{(2)} = n_{ij} - y_{ij}$. In order to compare the counts for all replicates $r = 1, \dots, R$ at the base (B) and the end (E) time points for each SNP position i , we denote $B_r = \{j | t_j = B, r_j = r\}$ and $E_r = \{j | t_j = E, r_j = r\}$. The CMH test statistic (see Agresti (2002) and Appendix A.1) compares the cell counts in Table 1 to their null expected value and follows a chi-squared distribution with one degree of freedom $\chi^2_{(df=1)}$. We performed CMH tests on the simulated and real data for each SNP position independently using the implementation of the software PoPoolation2 (Kofler *et al.*, 2011).

	Base gen. (B)	End gen. (E)	\sum
SNP i allele 1	$y_{iB_r}^{(1)}$	$y_{iE_r}^{(1)}$	$y_{i,r}^{(1)}$
SNP i allele 2	$y_{iB_r}^{(2)}$	$y_{iE_r}^{(2)}$	$y_{i,r}^{(2)}$
\sum	n_{iB_r}	n_{iE_r}	$n_{i,r}$

Table 1: 2×2 contingency table of allele counts for the r -th replicate for the CMH test.

2.7 Simulations

To evaluate the performance of the GP-based method we simulated data that mimics the dynamics of evolving *Dmel* populations at the genomic level. We carried out forward Wright-Fisher simulations of allele frequency trajectories of populations using the MimicrEE simulation tool (Kofler and Schlötterer, 2014). The initial haplotypes were taken from Kofler and Schlötterer (2014) and capture the natural variation of *Dmel* population. By sampling from the initial set we established $r = 5$ replicated base populations (with effective population size of about 200) and let each of them evolve for 60 generations at a constant size of 1000. The recombination rate was set at a predefined level, calculated by D. A. Petrov (Singh *et al.*, 2005). Low recombining regions were excluded from the simulations. We followed the evolution of the total number of 1,939,941 autosomal SNPs among which 100 were selected with rather strong selection coefficient of $s = 0.1$ and semi-dominance ($h = 0.5$). Furthermore, we required the selected SNPs to have a starting frequency in the range $[0.12, 0.8]$, not to lose the minor allele in the course of time due to drift. We recorded the nucleotide counts for every second generation and performed Poisson sampling with $\lambda = 45$ (overall mean coverage in Orozco-TerWengel *et al.*, 2012) on the count data to produce coverage information (see Appendix A.2). We repeated the whole simulation experiment three times each time using a different set of selected SNPs.

2.8 Evaluation Metrics

The methods were evaluated based on precision, recall and average precision (Manning *et al.*, 2008). Precision and recall are commonly used metrics for comparing the ranking-based methods which aim to get most of the relevant items in the very top of the ranked list of the items, in our case selected SNPs among top ranked SNPs. Precision is defined as the fraction of SNPs that are selected, and recall is defined as the fraction of selected SNPs that are returned. That is,

$$pre(k) = \frac{\text{number of selected SNPs in } k \text{ top SNPs}}{k} \quad (17)$$

$$rec(k) = \frac{\text{number of selected SNPs in } k \text{ top SNPs}}{\text{number of selected SNPs}}. \quad (18)$$

The curve obtained by plotting the precision at every position in the ranked sequence of items as a function of recall is called the precision-recall curve. The area under the curve can be summarised using the average precision (Manning *et al.*, 2008), which is defined as the average of $pre(k)$ after every returned selected SNP:

$$aveP = \frac{\sum_{k=1}^N (pre(k) \mathbb{1}_{sel}(k))}{\text{number of selected SNPs}}, \quad (19)$$

where N is the total number of SNPs and

$$\mathbb{1}_{sel}(k) = \begin{cases} 1, & \text{if item at rank } k \text{ is a selected SNP,} \\ 0, & \text{otherwise.} \end{cases} \quad (20)$$

3 Results

3.1 Simulated Data

We applied the BBGP and CMH methods to the simulated data with different numbers of time points (i.e., generations) and replicates. We started with nine time points $\{0, 6, 14, 22, 28, 38, 44, 50, 60\}$ and then removed the midpoint of the shortest interval until the desired number of time points was achieved. In the case of a tie, we kept the time point which is closest to the real sequenced time points (Orozco-TerWengel *et al.* (2012), see also Appendix A.3 for the complete list of time point sets used). We performed BBGP separately for each of the sampling schemes while CMH can only use two time points (first and last). All simulated SNPs were scored using Bayes factors for the BBGP, and p -values for the CMH test (see Figure 8 in the appendix for an example of a graphical visualisation of the scores).

To investigate the effect of the number of replicates, we chose $r = 2, 3, 4, 5$ replicates at each sampled time point. We first performed CMH tests with all possible r -replicate combinations. We then applied BBGP only to the best-performing replicate combinations of each size according to average precision in the CMH evaluations. This strategy ensures a fair comparison between the methods as BBGP is always evaluated against the best CMH results. We also compared BBGP to the standard GP of Kalaitzis and Lawrence (2011) that does not use the beta-binomial model variances using the same replicate combinations as BBGP but only 6 time points.

As shown in Figure 4 (see also Figure 9 in the appendix), BBGP achieves a higher average precision than the standard GP or the CMH. Somewhat surprisingly, CMH seems to benefit very

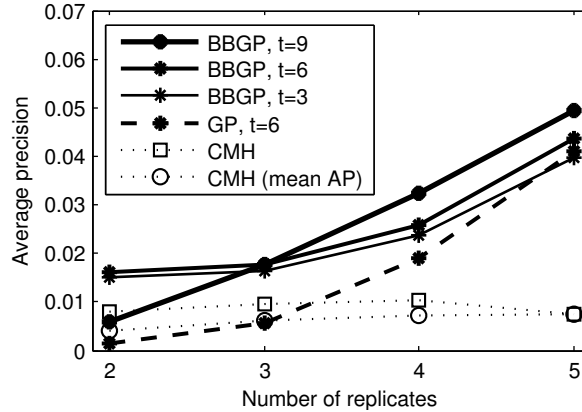


Figure 4: *Average precisions (AP) for CMH, BBGP, and standard GP with different number of replicates.* The used replicates have been selected as the best-performing r -replicate combinations in the CMH test, except for the CMH mean AP which has been computed by taking the mean of the average precisions over all r -replicate combinations for $r = 2, 3, 4, 5$.

little from more replicates while the performance of the GP methods improves significantly with more replicates. We observe that the CMH is very sensitive to the specific replicates included, as including the fifth replicate in the optimal sequence actually leads to worse performance than four replicates (Figure 9(d) in the appendix). We did not observe similar behaviour with the GP methods. On average over all possible r -replicate combinations adding more replicates helps the CMH as well. The performance of the standard GP approaches that of BBGP as the number of replicates increases, which is consistent with the view that the stronger prior information from sequencing depth is most important when the data are otherwise scarce, as is often the case in real experiments. The full precision recall curves corresponding to the results are shown in Figure 5 (see also Figure 9 in the appendix). While adding more replicates improves BBGP performance significantly, adding more time points helps at most very little (Figure 6). The running time needed to analyse 1000 SNPs in (4 replicates, 6 time points) setting is approximately 30 minutes on a desktop running Ubuntu 12.04 with Intel(R) Xeon(R) CPU E3-1230 V2 at 3.30GHz. The performance can also vary noticeably between different experiments depending on their difficulty (see Figure 10 in the appendix). For example, there is a 10-fold difference in AP between Experiment 1 and Experiment 3 for both methods (Figure 10 in the appendix, see also Kofler and Schlötterer (2014) for the CMH), but the BBGP-based test consistently outperforms the CMH test.

We also investigated if the two methods identify different types of selected SNPs. We calculated allele frequency change (AFC) for each SNP based on the average difference between the base and end populations across replicates. The CMH is very sensitive to large AFCs, while the candidates detected by the BBGP have a much more uniform distribution of AFCs (Figure 11 in the appendix). In general, we would expect a uniform distribution of AFC, as very large AFCs are only possible for SNPs with low starting frequency giving them the potential to rapidly increase. BBGP is much more accurate than CMH in all AFC classes as can be demonstrated by the performance breakdown (Figure 12 in the appendix).

3.2 Real Data Application

Orozco-TerWengel *et al.* (2012) applied the evolve and re-sequencing with HTS on *Dmel* popula-

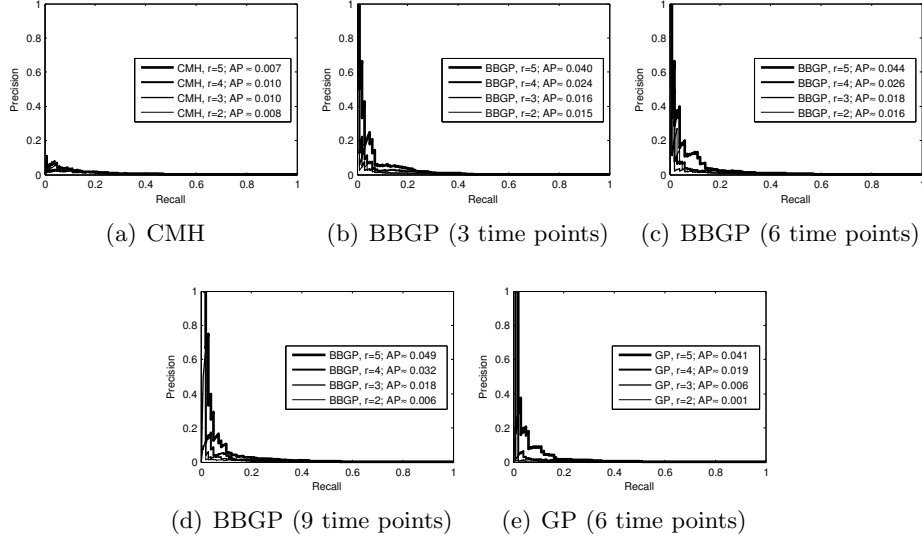


Figure 5: Full precision-recall curves for the CMH and BBGP methods in the situation of Figure 4.

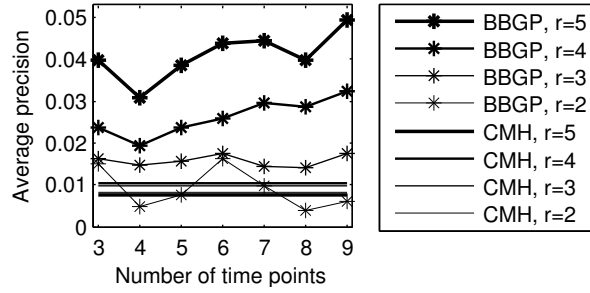


Figure 6: Average precisions (AP) for CMH and BBGP with different number of replicates and time points. More replicates are indicated by thicker lines. APs for the CMH are given as constant lines in order to facilitate the comparison (CMH is performed using only the first and last time points).

tions adapting to elevated temperature regime to identify evolutionary trajectories of selectively favoured alleles. They established replicated base populations from isofemale lines collected in Portugal. The populations were propagated at a constant size of 1000 for 37 generations under fluctuating temperature regime (12h at 18 °C and 12h at 28 °C). DNA pool of 500 females (Pool-Seq) was extracted and sequenced in multiple replicates at the following time points: three replicates at the base generation 0 (B); two replicates at generation 15, an additional replicate at generation 23 and at generation 27; three replicates at the end generation 37 (E).

CMH test was performed on a SNP-wise basis to identify significant allele frequency changes between the B and E populations (see Orozco-TerWengel *et al.* (2012) and Appendix A.4). We applied the BBGP method on 1,547,765 SNPs from the experiment and compared the results B-E comparison of the CMH test. The overlap between the top 2000 candidate SNPs of the CMH and the BBGP was rather small (524 SNPs). However, the peaks of both methods covered the same regions (Figure 7). Although *Dmel* generally has rather small levels of linkage, linkage disequilibrium might have built up during the course of the experiment. In fact, linkage

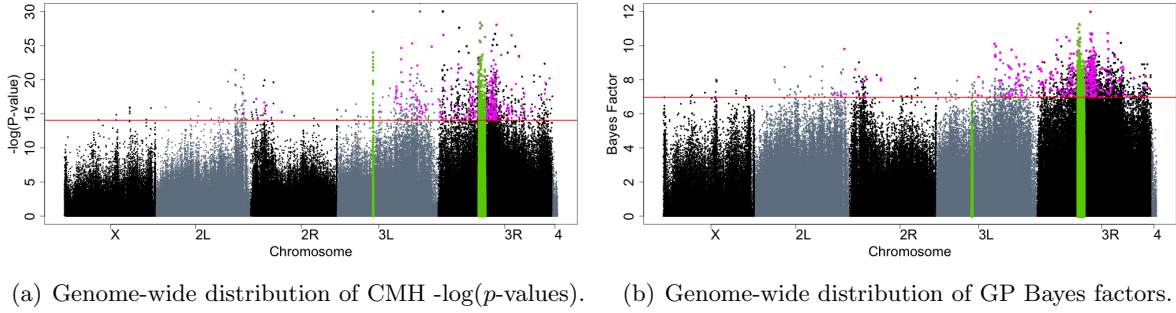


Figure 7: *Manhattan plots of genome-wide SNP-values.* (a) $-\log(p\text{-values})$ for the CMH test B-E comparison. Only SNPs with p -values up to $-\log_{10}(1e-30)$ are shown; 3 SNPs with p -values above are set to $-\log_{10}(1e-30)$ on the plot. (b) Bayes factors for the BBGP. Only those SNPs are indicated for which we calculated both the p -values and the Bayes factors (we did not infer Bayes factors for fixed SNPs). A 1 Mb region was excluded from the analysis on 3R as a low frequency haplotype spreads during the experiment due to an inversion. Previously, the chorion gene cluster on 3L was also excluded as this region has extremely high coverage (Orozco-TerWengel *et al.*, 2012). Regions that were excluded from the analysis are shown in green. The red horizontal line indicates the top 2000 candidate cutoff. The common candidates among the top 2000 are highlighted in magenta. Figure (b) shows well how the beta-binomial variance control can handle high coverage problem of the excluded region on 3L.

disequilibrium had a major effect on the number of candidate SNPs identified by the CMH as well as the BBGP based test. As the flanking SNPs showed signs of hitchhiking, the observed AFC of the flanking SNPs were also significant (see also Manhattan plot for the simulated SNPs, Figure 8 in the appendix) and made it difficult to narrow down functionally important regions for thermoadaptation.

3.2.1 Gene Ontology Enrichment

We used Gowinda (Kofler and Schlötterer, 2012) to test for the enrichment of functional categories according to the Gene Ontology (GO) database (Ashburner *et al.*, 2000). Gowinda tests significance of overrepresentation of candidate SNPs in each GO category. It uses permutation tests to eliminate potential sources of bias caused by difference of gene length and genes that overlap. We tested the top 2000 candidate SNPs for both the CMH and the BBGP methods, respectively. FDR correction was applied on the inferred p -values to account for multiple testing. Using Gowinda we did only find one significant category ($p < 0.05$) for the BBGP and no significant categories for the CMH test (see Table 3 and Table 4 in the appendix).

In addition to taking an arbitrary threshold of the top 2000 SNPs, we also considered the full distributions of p -values for the CMH and the distribution of Bayes factors for the BBGP based tests. For each GO category we compared distribution of all SNP-values (p -values for the CMH and Bayes factors for the GP) in that GO gene set to the distribution outside that gene set using a one-tailed Mann-Whitney U test (MWU) as applied by Segrè *et al.* (2010). Similar to Gowinda, we used permutations to account for biases such as gene length and other confounding effects (see Appendix A.5). We also conserve the gene order during the randomisation as functionally similar genes are often clustered nearby on a chromosome. Using the MWU tests, we found significant GO category enrichments for both methods (Table 2 and Figure 13 in the appendix).

Emp. p-val	≤ 0.1	≤ 0.05	≤ 0.01
CMH	84	37	4
BBGP	74	30	5
Common	59	15	3

Table 2: *The number of enriched GO categories for the MWU test.* Empirical p -values (Emp. p -val.) are based on 1000 permutations. Overlap between CMH and BBGP tests are shown for different significance levels: $p \leq 0.1$, $p \leq 0.05$ and $p \leq 0.01$. With FDR correction there were no significantly enriched categories.

Moreover, the top ranked candidate categories were similar in both cases (see Table 5 and Table 6 in the appendix). There is a significant overlap between the discovered categories, but there are also clear differences.

4 Discussion

Our results in detecting SNPs that are evolving under selection using a GP model presented in this paper clearly demonstrate the importance of careful modelling of the measurement uncertainty through a good noise model, in our case using the beta-binomial model of sequencing data. Especially when data are scarce, the BBGP approach leads to much higher accuracy than standard maximum likelihood estimation of noise variances. Incorporating the non-Gaussian likelihood directly to the GP would also be possible, but it would lead to computationally more demanding inference.

In terms of experimental design, the most effective way to improve performance is to collect more replicate measurements. Compared to the CMH test, the BBGP is clearly superior in utilising more replicates. We suspect this is because CMH assumes all replicates should have similar odds ratios between the two time points and this is not sufficiently satisfied by the noisy data. On the other hand, the benefit of adding more intermediate data points seems marginal. This may be because the shape of selected trajectories is a simple sigmoid and adding more points provides limited help in estimating them.

The presented GP-based test is sensitive to SNPs with a consistent time-varying profile. A statistically more accurate model could be derived by assuming each replicate to follow an independent GP, but this would lead to a less sensible test as it would also pick up SNPs with strong but inconsistent drift. Exploring hierarchical GP models to capture the correct dependence structure in a sensible test is an interesting avenue of future research.

In a whole-genome experiment, linkage disequilibrium between nearby markers is an important confounder in identifying the selected marker. None of the methods tested takes this into account, which introduces the problem of hitchhikers, i.e. markers that behave like they would be selected because they are strongly linked with a truly selected marker. It is possible to incorporate such information into the GP model at the cost of higher computational complexity, and this is clearly an important avenue of future research. This is potentially a further advantage of the GP, because it is not possible to incorporate this into frequentist tests.

5 Conclusion

In this paper, we developed a new test that is based on combining GP models with a beta-binomial model of sequencing data, and compared it with the CMH test that allows the pairwise comparison of base and evolved populations across several replicates.

Our results demonstrate that GP models are well-suited for analysing quantitative genomic time series data because they can effectively utilise the available data, making good use of additional time points and replicates unhindered by uneven sampling and consistently show performance superior to the CMH test.

The GP framework is very flexible which enables extensions utilising for example linkage disequilibrium over nearby alleles. As GP models can easily incorporate additional information on the data, we envisage that further promising combinations of the GP approach with evolutionary models will emerge.

Acknowledgement

C.K. would like to thank the Institute of Pure and Applied Mathematics (IPAM) for a stay at Genomics programme at which the idea of working on evolutionary time series data evolved.

Funding: The work was supported under the European ERASysBio+ initiative project “SYNERGY” through the Academy of Finland [135311]. A.H. was also supported by the Academy of Finland [259440]. A.J. is member of the Vienna Graduate School of Population Genetics which is supported by a grant of the Austrian Science Fund (FWF) [W1225-B20].

References

- Agresti, A. (2002). *Categorical Data Analysis*. Wiley, New York.
- Äijö, T et al. (2013). Sorad: a systems biology approach to predict and modulate dynamic signaling pathway response from phosphoproteome time-course measurements. *Bioinformatics*, **29**(10), 1283–1291.
- Ashburner, M et al. (2000). Gene ontology: tool for the unification of biology. *Nat Genet*, **25**(1), 25–29.
- Barrick, JE et al. (2009). Genome evolution and adaptation in a long-term experiment with escherichia coli. *Nature*, **461**(7268), 1243–1247.
- Burke, M et al. (2010). Genome-wide analysis of a long-term evolution experiment with Drosophila. *Nature*, **467**, 587–590.
- Burke, M. K. and Long, A. (2012). What paths do advantageous alleles take during short-term evolutionary change? *Molecular Ecology*, **21**, 4913–416.
- Cooke, EJ et al. (2011). Bayesian hierarchical clustering for microarray time series data with replicates and outlier measurements. *BMC Bioinformatics*, **12**, 399.
- Gao, P et al. (2008). Gaussian process modelling of latent chemical species: applications to inferring transcription factor activities. *Bioinformatics*, **24**(16), i70–i75.
- Hensman, J et al. (2013). Hierarchical Bayesian modelling of gene expression time series across irregularly sampled replicates and clusters. *BMC Bioinformatics*, **14**, 252.
- Honkela, A et al. (2010). Model-based method for transcription factor target identification with limited data. *Proc Natl Acad Sci U S A*, **107**(17), 7793–7798.
- Illingworth, CJR et al. (2012). Quantifying selection acting on a complex trait using allele frequency time series data. *Mol Biol Evol*, **29**(4), 1187–1197.

- Jones, N. S. and Moriarty, J. (2013). Evolutionary inference for function-valued traits: Gaussian process regression on phylogenies. *J R Soc Interface*, **10**(78), 20120616.
- Kalaitzis, A. A. and Lawrence, N. D. (2011). A simple approach to ranking differentially expressed gene expression time courses through Gaussian process regression. *BMC Bioinformatics*, **12**, 180.
- Kawecki, T.J et al. (2012). Experimental evolution. *Trends Ecol Evol*, **27**(10), 547–560.
- Kimura, M. (1962). On the probability of fixation of mutant genes in a population. *Genetics*, **47**, 713–719.
- Kirk, P. D. W. and Stumpf, M. P. H. (2009). Gaussian process regression bootstrapping: exploring the effects of uncertainty in time course data. *Bioinformatics*, **25**(10), 1300–1306.
- Kofler, R. and Schlötterer, C. (2012). Gowinda: unbiased analysis of gene set enrichment for genome-wide association studies. *Bioinformatics*, **28**, 2084–2085.
- Kofler, R. and Schlötterer, C. (2014). A guide for the design of evolve and resequencing studies. *Mol Biol Evol*, **31**(2), 474–483.
- Kofler, R et al. (2011). PoPoolation2: identifying differentiation between populations using sequencing of pooled DNA samples (Pool-Seq). *Bioinformatics*, **27**, 3435–3436.
- Lang, GI et al. (2013). Pervasive genetic hitchhiking and clonal interference in forty evolving yeast populations. *Nature*, **500**(7464), 571–574.
- Liu, Q et al. (2010). Estimating replicate time shifts using Gaussian process regression. *Bioinformatics*, **26**(6), 770–776.
- Liu, W. and Niranjan, M. (2012). Gaussian process modelling for bicoid mRNA regulation in spatio-temporal Bicoid profile. *Bioinformatics*, **28**(3), 366–372.
- Manning, CD et al. (2008). *Introduction to Information Retrieval*. Cambridge University Press.
- Orozco-TerWengel, P et al. (2012). Adaptation of *Drosophila* to a novel laboratory environment reveals temporally heterogeneous trajectories of selected alleles. *Molecular Ecology*, **21**, 4931–4941.
- Palacios, J. A. and Minin, V. N. (2013). Gaussian process-based Bayesian nonparametric inference of population size trajectories from gene genealogies. *Biometrics*, **69**(1), 8–18.
- Rasmussen, C. E. and Williams, C. K. I. (2006). *Gaussian Processes for Machine Learning*.
- Segrè, A et al. (2010). Common inherited variation in mitochondrial genes is not enriched for associations with type 2 diabetes or related glycemic traits. *PLoS Genet.*, **6**, e1001058. doi:10.1371/journal.pgen.1001058.
- Singh, N et al. (2005). Genomic heterogeneity of background substitutional patterns in *Drosophila melanogaster*. *Genetics*, **169**, 709–722.
- Stegle, O et al. (2010). A robust Bayesian two-sample test for detecting intervals of differential gene expression in microarray time series. *J Comput Biol*, **17**(3), 355–367.
- Titsias, MK et al. (2012). Identifying targets of multiple co-regulating transcription factors from expression time-series by Bayesian model comparison. *BMC Syst Biol*, **6**, 53.
- Turner, T et al. (2011). Population-based resequencing of experimentally evolved populations reveals the genetic basis of body size variation in *Drosophila melanogaster*. *PLoS Genetics*, **7**(3), e1001336.
- Yuan, M. (2006). Flexible temporal expression profile modelling using the Gaussian process. *Comput. Statist. Data Anal.*, **51**(3), 1754–1764.
- Zhou, D et al. (2011). Experimental selection of hypoxia-tolerant *Drosophila melanogaster*. *Proceedings of the National Academy of Sciences*, **7**(108), 2349–2354.

A Supplementary Methods

A.1 Cochran-Mantel-Haenszel Test

SNPs with consistent change in allele frequency were identified by Cochran-Mantel-Haenszel test (CMH) by Orozco-TerWengel *et al.* (2012). The CMH test is an extension of testing equivalence of proportions (implies that the odds ratio is 1) in a 2×2 contingency table to replicated tables sampled from the same underlying population. The estimate for the joint odds ratio in the replicated $2 \times 2 \times R$ tables ($r = 1, \dots, R$, Table 1) is tested for difference from 1.

We follow the definition of the CMH by Agresti (2002). Allele counts for the different replicates ($y_{iB_r}^{(1)}$, Main Text, Table 1) are assumed to be independent. Under the null hypothesis they follow a hypergeometric distribution with mean and variance:

$$E(y_{iB_r}^{(1)}) = \frac{y_{i,r}^{(1)} n_{iB_r}}{n_{i,r}}$$

$$V(y_{iB_r}^{(1)}) = \frac{y_{i,r}^{(1)} y_{i,r}^{(2)} n_{iB_r} n_{iE_r}}{n_{i,r}^2 (n_{i,r} - 1)}.$$

The test statistics compares $\sum_r y_{iB_r}^{(1)}$ to its null expected value by combining information from R partial tables:

$$CMH = \frac{\left[\sum_r \left(y_{iB_r}^{(1)} - E(y_{iB_r}^{(1)}) \right) \right]^2}{\sum_r Var \left(y_{iB_r}^{(1)} \right)}.$$

This statistic approximately follows a chi-square distribution with one degree of freedom $\chi_{(df=1)}^2$. Under the null hypothesis, we assume independence of the start (B) and end (E) time points of the experiment for each replicate. Thus, the odds ratio for each replicate is approximately one. When the odds ratios in each partial table is significantly different from one (dependence) we expect the nominator in the test statistic to be large in absolute value.

A.2 Simulations

We carried out forward Wright-Fisher simulations of allele frequency (AF) trajectories of evolving populations with MimicrEE (Kofler and Schlötterer, 2014). The founder population was generated using 8000 simulated haploid genomes from Kofler and Schlötterer (2014). Out of the 8000 genomes 200 were sampled to establish a diploid base population of 1000 individuals (sampled out of the 200 with replacement). The base population contains only autosomal SNPs. Low recombining regions ($< 1cM/Mb$) were also excluded from the simulations (for more information see Kofler and Schlötterer, 2014). We placed 100 selected SNPs randomly in the base population with selection coefficient, $s = 0.1$ and semi-dominance, $h = 0.5$, selected from SNPs with starting allele frequency in the range $[0.12, 0.8]$. We applied this restriction on the starting AF to increase the probability of fixation of the selected allele. According to population genetics theory the probability of fixation is $P_{fix} = (1 - e^{-2N_e s p}) / (1 - e^{-2N_e s})$ (Kimura, 1962), where N_e is the effective population size, s is the selection coefficient and p is the starting allele frequency. Taking the base population of 1000

homozygote individuals and the set of selected SNPs we followed the simulation protocol outlined at <https://code.google.com/p/mimicree/wiki/ManualMimicreeSummary> for 5 replicates independently. As described in Kofler and Schlötterer (2014), we aimed to reproduce the sampling properties of Pool-Seq using Poisson sampling with $\lambda = 45$ (using the script `poisson-3fold-sample.py` available at <http://mimicree.googlecode.com>). Briefly, we considered coverage differences between samples, coverage fluctuations due to GC-bias and stochastic sampling heterogeneity.

A.3 Performance tests with different numbers of time points and replicates

We measured the performance of the BBGP and the CMH test on the simulated data sets using various number of time points and replicates. To test the performance improvement with increasing number of time points we carried out the BBGP on the following sets of generations:

- 3 time points: 0, 38, 60,
- 4 time points: 0, 14, 38, 60,
- 5 time points: 0, 14, 28, 38, 60,
- 6 time points: 0, 14, 28, 38, 50, 60,
- 7 time points: 0, 14, 22, 28, 38, 50, 60,
- 8 time points: 0, 6, 14, 22, 28, 38, 50, 60,
- 9 time points: 0, 6, 14, 22, 28, 38, 44, 50, 60.

For the CMH test, however, we always performed a base-end (generation 60) comparison, because the CMH is a pairwise statistic. The genome-wide test statistic values are shown in Figure 8, for the BBGP (6 time points) and the CMH for 5 replicates as an example. The effects of different numbers of replicates on the performance of the proposed methods are shown in Figure 9, using precision recall curves along with average precisions.

We carried out 3 independent runs of simulations with different sets of selected SNPs but keeping the parameters unchanged (Figure 10). Finally, we compared with a performance break down according to Allele Frequency Change (AFC) the BBGP to CMH test in different AFC classes (Figure 11 and Figure 12).

A.4 Real Data Application

We applied the BBGP on HTS data of experimentally evolved *D. melanogaster* populations (Orozco-TerWengel *et al.*, 2012). We compared our proposed method to the CMH results coming from the B-E comparison, downloaded from Dryad database (<http://datadryad.org>) under the accession: doi: 10.5061/dryad.60k68. We used the synchronized pileup files (BF37.sync) which contains a total number of 1,547,837 SNPs. The CMH test was only performed on SNPs that met certain quality criteria regarding the minor allele count and the maximum coverage (for more information on SNP calling please consult Orozco-TerWengel *et al.*, 2012).

A.5 Gene Set Enrichment

For a biologically meaningful comparison of the CMH test and the BBGP test we performed a gene set enrichment analysis. Below we explain how we used the tool Gowinda (Kofler and Schlötterer, 2012) for Gene Ontology enrichment and how we extended it.

A.5.1 Gene Set Enrichment with Gowinda

Gowinda counts the number of genes (set of candidate genes) that contain candidate SNPs. Then, assuming that SNPs are in complete linkage within the same gene, it randomly samples SNPs from the pool of all SNPs until the number of corresponding genes is equal to the cardinality of the set of candidate genes. This step is repeated several times and from the resulting random set of genes an empirical null distribution of candidate gene abundance is calculated for each gene set. The significance level of enrichment for each gene set is inferred by counting the randomly drawn cases, in which there were more candidate genes present than in the original candidate gene set. Gowinda requires the following input files: annotation file containing the annotation of species of interest; gene set file of the associated genes (e.g. Gene Ontology (GO) association file); list of SNP-value pairs as the output of our analysis; list of candidate SNPs, which is a subset of all SNP-value pairs that we define as candidates according to some predetermined condition. We used the following inputs: the annotation file of *Drosophila melanogaster* version 5.40 downloaded from Flybase (<http://flybase.org/>); the GO association file was obtained from R Bioconductor GO.db package version 2.9.0 (accessed at 05/03/2013). We took the top 2000 candidate SNPs for both methods as candidate SNPs and run Gowinda with the following parameters: `--simulations 10000000 --gene-definition updownstream200 --mode gene`. We also took 200 base pairs up- and downstream regions from the gene boundaries into the analysis. For more details please see Kofler and Schlötterer (2012).

Using Gowinda led to only one significantly enriched category for the BBGP and no significant enrichment for the CMH test ($FDR < 0.05$; top ranked categories in Table 3, Table 4).

A.5.2 Gene Set Enrichment with Mann-Whitney U Test

For using Gowinda we had to fix a threshold above which we consider a SNP as a possible candidate. Defining this threshold can be arbitrary, changes in the threshold can result in different enriched gene sets. Therefore, we decided to compare the distribution of all SNP-values in a specific gene set to the distribution outside that gene set using Mann-Whitney U test (MWU). This test allows us to decide if a particular gene set is significantly enriched based only on the ranks of SNP-values in that set.

We performed the MWU test similarly as Segrè *et al.* (2010). We used the previously mentioned gene set file obtained from R Bioconductor GO.db package; and a list of all SNPs with the corresponding values (output of the tests). For mapping the SNPs to the genes we used SNPEFF 2.0.1 (<http://snpeff.sourceforge.net/>). For each gene set we summarized the list of SNPs present in that particular set and created a vector of corresponding SNP-values (list of p -values or Bayes factors). Then we tested the alternative hypothesis that the distribution of these values is skewed towards the extreme values (low ranked p -values for the CMH, high ranked Bayes factors for the GP) compared to the values among the rest of the SNPs. This gives the observed rank-sum p -value for the investigated gene set. Then, similarly to Gowinda, we performed permutations to account for biases by simulating random gene sets (but keeping the chromosomal order) with identical size as observed. For every round of simulation we calculated the ranked-sum p -values as before. Finally, an expected rank-sum p -value was computed from this null distribution, as the fraction of randomly sampled gene sets whose rank-sum p -value was less than or equal to the observed rank-sum p -value of the gene set.

The top ranked significant enrichments calculated with MWU test using 1000 permutations are functionally rather similar. Figure 13 shows the overlap between highly enriched categories for

different empirical p -value cutoffs. The categories are listed in Table 5 and Table 6.

B Supplementary Tables and Figures

GO category	p -Value	FDR	Description
GO:0004003	0.000074	0.0630949	ATP-dependent DNA helicase activity
GO:0008094	0.0001048	0.0630949	DNA-dependent ATPase activity
GO:0006281	0.0002248	0.097873567	DNA repair
GO:0046914	0.000305	0.1027073	transition metal ion binding

Table 3: *Top ranked GO enrichment results with Gowinda on the CMH candidates.* Only the top 4 categories are shown.

GO category	p -Value	FDR	Description
GO:0005506	0.0000143	0.015987	iron ion binding
GO:0015671	0.0004199	0.256548725	oxygen transport
GO:0004252	0.0006096	0.256548725	serine-type endopeptidase activity
GO:0004989	0.0007332	0.256548725	octopamine receptor activity

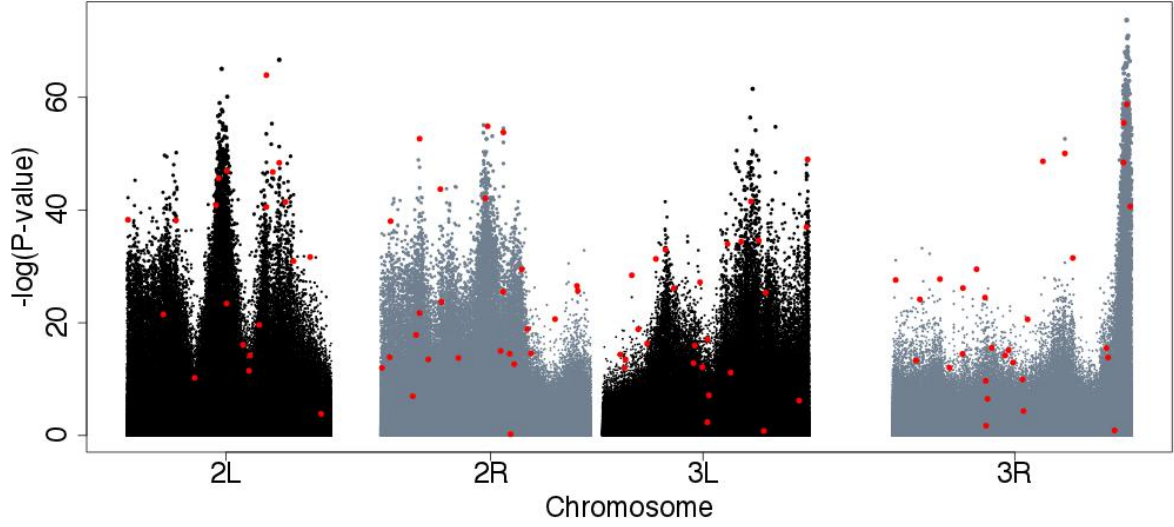
Table 4: *Top ranked GO enrichment results with Gowinda on the BBGP candidates.* Only the top 4 categories are shown.

GO category	Obs. p-val.	Emp. p-val.	Description
GO:0007274	2.8543e-156	0.001	neuromuscular synaptic transmission
GO:0032504	3.2726e-49	0.001	multicellular organism reproduction
GO:0006997	1.2159e-17	0.001	nucleus organization
GO:0007379	4.9304e-75	0.008	segment specification
GO:0003774	1.8303e-19	0.011	motor activity
GO:0009792	5.8937e-30	0.013	embryo development ending in birth or egg hatching
GO:0001700	9.7049e-31	0.015	embryonic development via the syncytial blastoderm
GO:0045451	4.5162e-20	0.015	pole plasm oskar mRNA localization
GO:0060810	2.3554e-19	0.015	intracell. mRNA loc. inv. in pattern specification proc.
GO:0060811	1.9679e-19	0.016	intracell. mRNA loc. inv. in anterior/posterior axis spec.
GO:0000975	1.5011e-32	0.017	regulatory region DNA binding
GO:0008298	5.7685e-17	0.017	intracellular mRNA localization
GO:0016573	3.4293e-08	0.024	histone acetylation
GO:0019094	6.8648e-19	0.025	pole plasm mRNA localization
GO:0060438	9.6931e-101	0.026	trachea development
GO:0000086	1.0455e-15	0.027	G2/M transition of mitotic cell cycle
GO:0030554	9.0394e-19	0.028	adenyl nucleotide binding
GO:0051049	4.8523e-52	0.029	regulation of transport
GO:0004386	1.9648e-09	0.029	helicase activity
GO:0007093	6.4409e-08	0.029	mitotic cell cycle checkpoint
GO:0032879	3.4419e-34	0.03	regulation of localization
GO:0060439	6.0698e-78	0.032	trachea morphogenesis
GO:0019904	3.6125e-74	0.032	protein domain specific binding
GO:0007350	1.1101e-25	0.033	blastoderm segmentation
GO:0000976	3.9652e-14	0.035	transcr.regulatory reg. sequence-spec. DNA binding
GO:0000977	2.8459e-28	0.037	RNA polymerase II reg. reg.seq.-spec. DNA binding
GO:0007276	3.7400e-24	0.038	gamete generation
GO:0007269	1.1198e-94	0.04	neurotransmitter secretion
GO:0004888	2.9136e-19	0.043	transmembrane signaling receptor activity
GO:0000981	1.9244e-28	0.044	seq.-spec DNA binding RNA pol. II transcr. factor activity
GO:0008306	1.2419e-35	0.046	associative learning
GO:0008355	6.2395e-32	0.047	olfactory learning
GO:0001012	1.3174e-37	0.048	RNA polymerase II regulatory region DNA binding
GO:0048149	1.6131e-23	0.048	behavioral response to ethanol
GO:0045664	7.9648e-23	0.048	regulation of neuron differentiation
GO:0010389	1.8391e-08	0.05	regulation of G2/M transition of mitotic cell cycle
GO:0009055	7.5572e-05	0.05	electron carrier activity

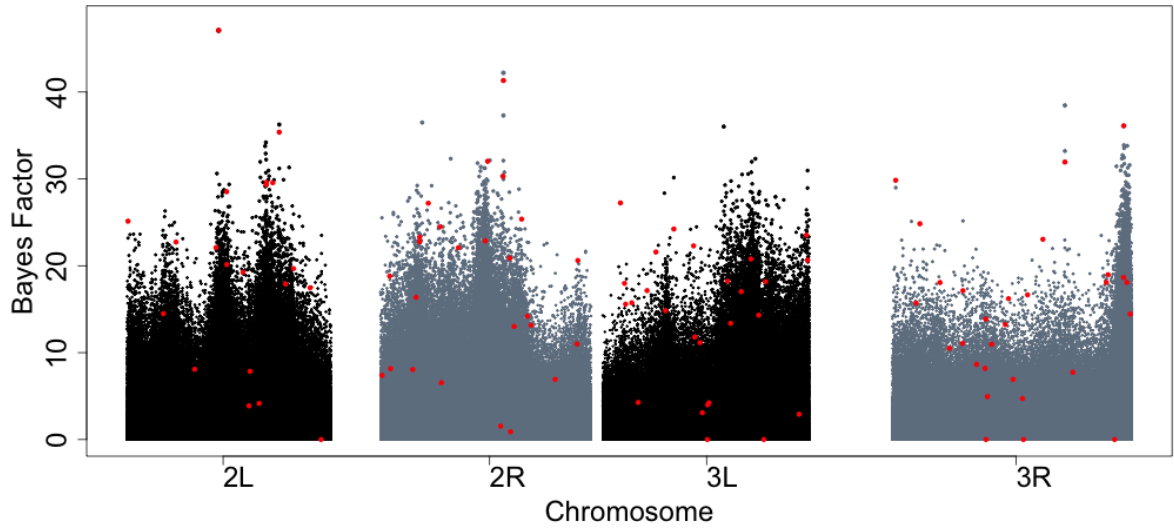
Table 5: *Results of the GO enrichment with MWU on the CMH candidates.* Only the categories are shown for which the empirical p -value ≤ 0.05 calculated for 1000 permutations.

GO category	Obs. p-val.	Emp. p-val.	Description
GO:0006997	4.1404e-19	0	nucleus organization
GO:0007274	1.0657e-130	0.002	neuromuscular synaptic transmission
GO:0007379	3.7449e-85	0.002	segment specification
GO:0032879	8.0269e-38	0.006	regulation of localization
GO:0000075	1.9450e-19	0.007	cell cycle checkpoint
GO:0000785	9.1310e-15	0.014	chromatin
GO:0051049	6.3596e-52	0.019	regulation of transport
GO:0009152	2.7329e-41	0.02	purine ribonucleotide biosynthetic process
GO:0006164	5.9106e-46	0.022	purine nucleotide biosynthetic process
GO:0004386	1.0113e-09	0.025	helicase activity
GO:0005179	1.9714e-16	0.026	hormone activity
GO:0000975	2.2740e-25	0.027	regulatory region DNA binding
GO:0000977	9.8625e-36	0.028	RNA pol. II regulatory reg. seq.-spec. DNA binding
GO:0000976	2.6106e-18	0.029	transcr. reg. region sequence-spec. DNA binding
GO:0001012	2.0242e-42	0.029	RNA polymerase II regulatory region DNA binding
GO:0030554	1.9638e-14	0.03	adenyl nucleotide binding
GO:0046914	5.2243e-27	0.032	transition metal ion binding
GO:0055114	7.0135e-18	0.032	oxidation-reduction process
GO:0005829	1.0637e-17	0.033	cytosol
GO:0019725	2.3293e-26	0.034	cellular homeostasis
GO:0032504	8.4897e-21	0.036	multicellular organism reproduction
GO:0009165	8.8494e-25	0.038	nucleotide biosynthetic process
GO:0008285	7.1838e-19	0.041	negative regulation of cell proliferation
GO:0007269	1.6094e-94	0.043	neurotransmitter secretion
GO:0010389	3.4665e-07	0.043	regulation of G2/M transition of mitotic cell cycle
GO:0031226	5.5250e-27	0.043	intrinsic to plasma membrane
GO:0032940	3.7154e-73	0.045	secretion by cell
GO:0017076	5.6881e-12	0.046	purine nucleotide binding
GO:0000086	5.0627e-14	0.048	G2/M transition of mitotic cell cycle
GO:0016491	1.1667e-10	0.048	oxidoreductase activity

Table 6: *Results of the GO enrichment with MWU on the BBGP candidates.* Only the categories are shown for which the empirical p -value ≤ 0.05 calculated for 1000 permutations.

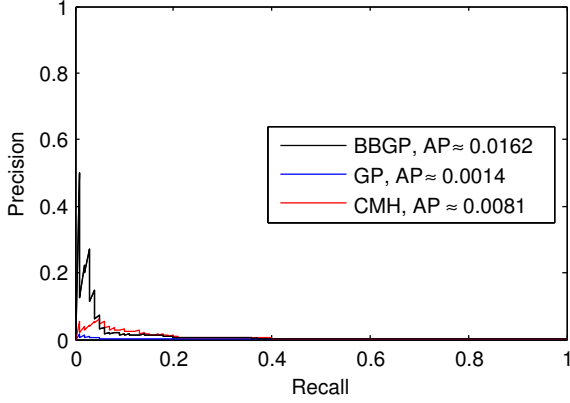


(a) Simulated data, genome-wide distribution of CMH $-\log(p\text{-values})$.

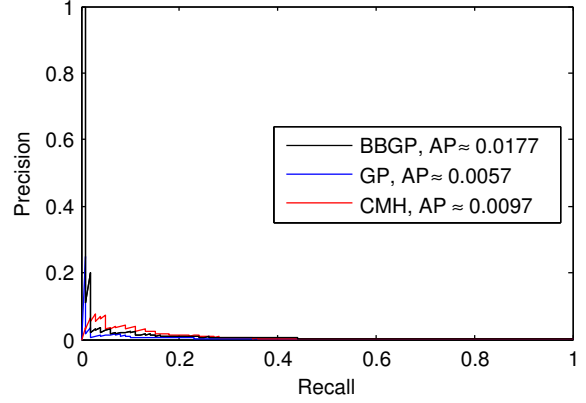


(b) Simulated data, genome-wide distribution of BBGP Bayes factors.

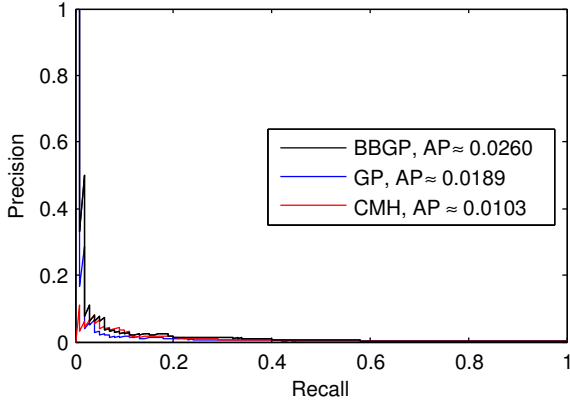
Figure 8: *Manhattan plots of genome-wide test statistic values on simulated data with 5 replicates.* (a) $-\log(p\text{-values})$ for the CMH test B-E comparison. (b) Bayes factors for the BBGP using 6 time points. Only autosomal regions were simulated and low recombining regions ($< 1\text{cM}/\text{Mb}$) were excluded. The 100 truly selected SNPs ($s=0.1$) are indicated in red. As the consequence of linkage structure we observe extended peaks in the vicinity of selected SNPs. However, there are still some truly selected SNPs that do not show clear pattern of frequency increase. A possible explanation for that can be that the time course, i.e. 60 generations, is not enough for them to rise in frequency. They can also interfere with each other and non-selected SNPs. Modeling spacial structure would be required to capture such a pattern.



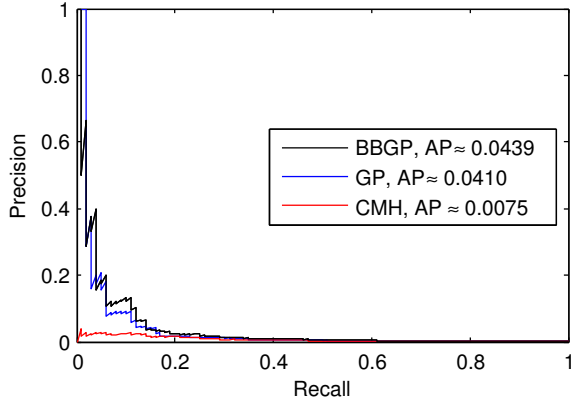
(a) Number of replicates: 2



(b) Number of replicates: 3

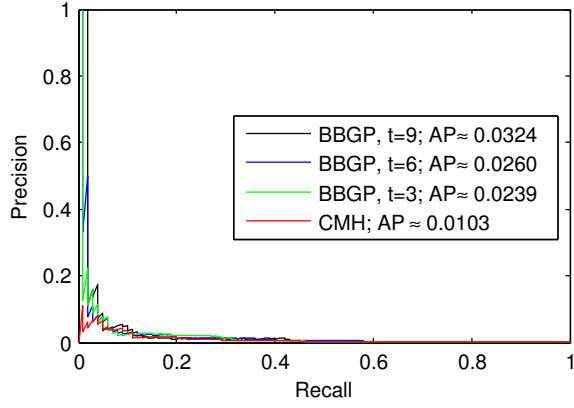


(c) Number of replicates: 4

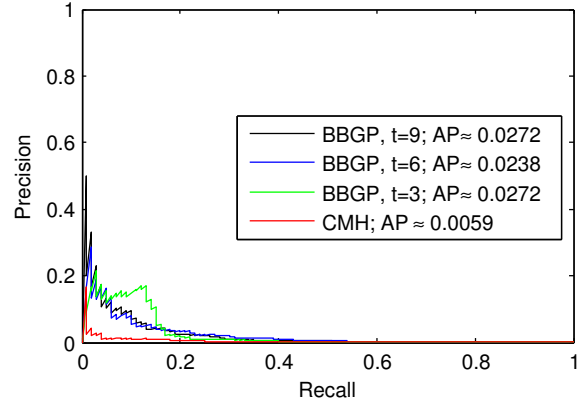


(d) Number of replicates: 5

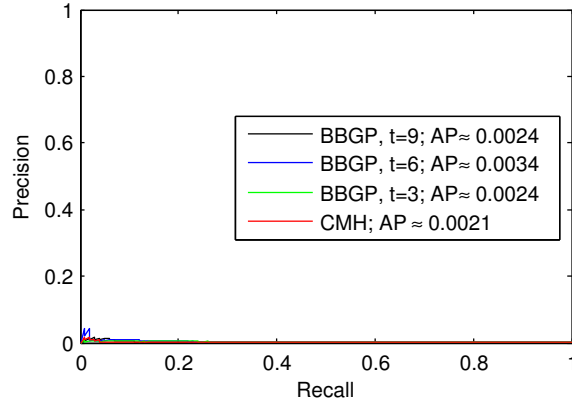
Figure 9: *Precision recall curves comparing CMH method to the standard GP and BBGP methods using different number of replicates and 6 time points.* Incorporation of the beta-binomial posterior variances into the GP model provides the most benefit when the number of replicates are small. The more replication is performed during the experiments the better performance can be expected from the GP-based methods. The CMH test, however, does not benefit from more replicates in the same way.



(a) Experiment: 1



(b) Experiment: 2



(c) Experiment: 3

Figure 10: *Precision recall curves comparing CMH to BBGP for 3 independent experiments.* The performance can vary noticeably between experiments (e.g., factor of 10 difference in AP between Experiment 1 and 3). Nevertheless, the BBGP based test consistently outperforms the CMH test.

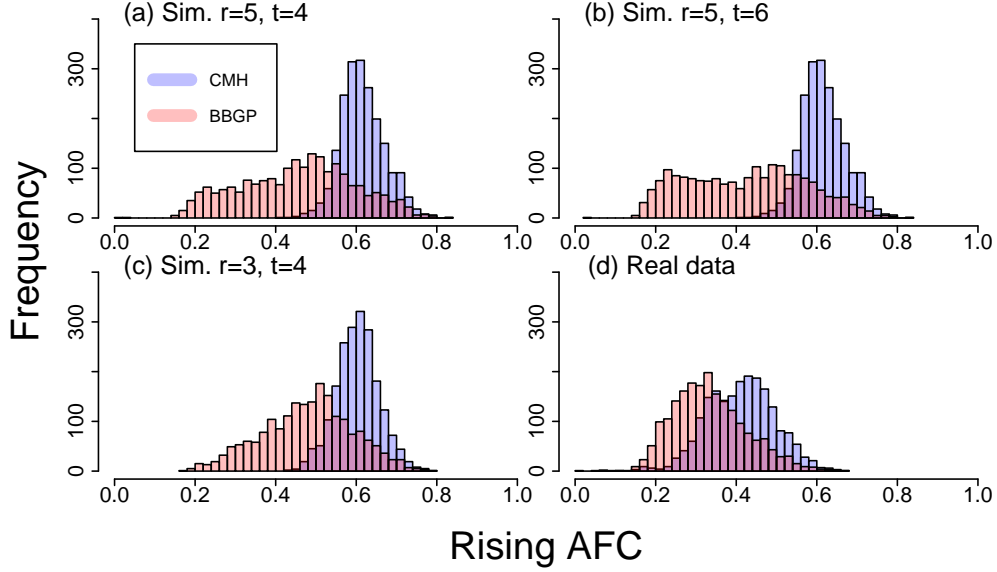


Figure 11: *Distribution of the average allele frequency change (AFC) of the rising allele for the top 2000 candidates.* AFC was calculated for each SNPs based on the average difference between the base and end populations across replicates. (a-b) AFC of the top 2000 candidates of the simulated data with 5 replicates, GP is performed on 4 (a) and 6 (b) time points, respectively. (c) AFC of the top 2000 candidates of the simulated data with 3 replicates, GP is performed on 4 time points. (d) AFC of the top 2000 candidates of the real data. We observed a significant location shift between the AFC distributions among the top 2000 candidate SNPs of the CMH and the BBGP (Mann-Whitney U, p -value $< 2.2e-16$ for all panels). The location shift indicates that the CMH test mostly captures radical AFC while the GP-based methods are also sensitive to consistent signals coming from intermediate time points.

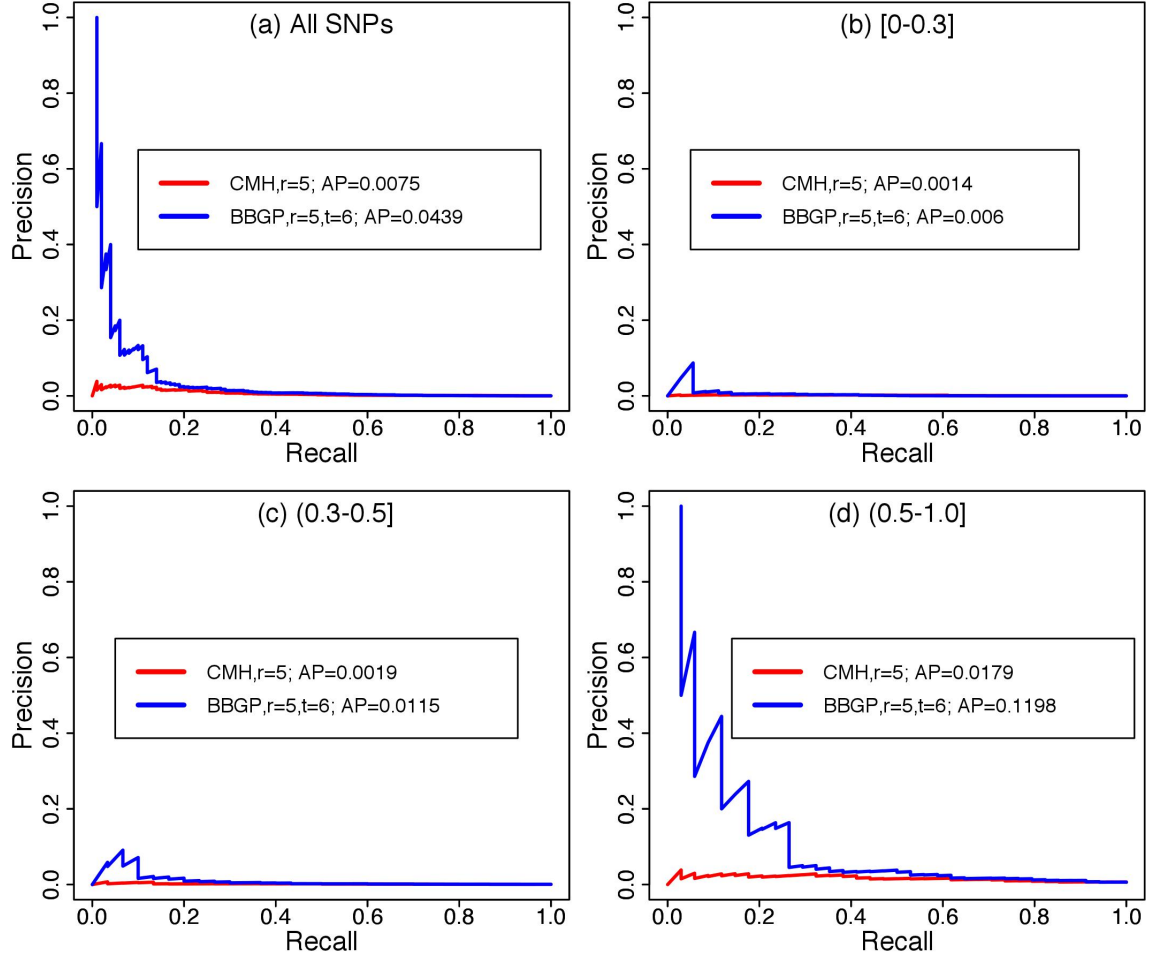


Figure 12: *Precision recall curves for different AFC classes.* The performance in terms of precision and recall is shown for the CMH and the BBGP in classes of SNPs with different allele frequency change. The AFC is measured between the base and end generations (60) and averaged over 5 replicates. For the BBGP 6 time points were used. Panel (a) shows the overall performance. For Panel (b)-(d), the AFC classes contain the following number of selected SNPs: 36 in class [0-0.3], 30 in class (0.3-0.5], 34 in class (0.5-1.0].

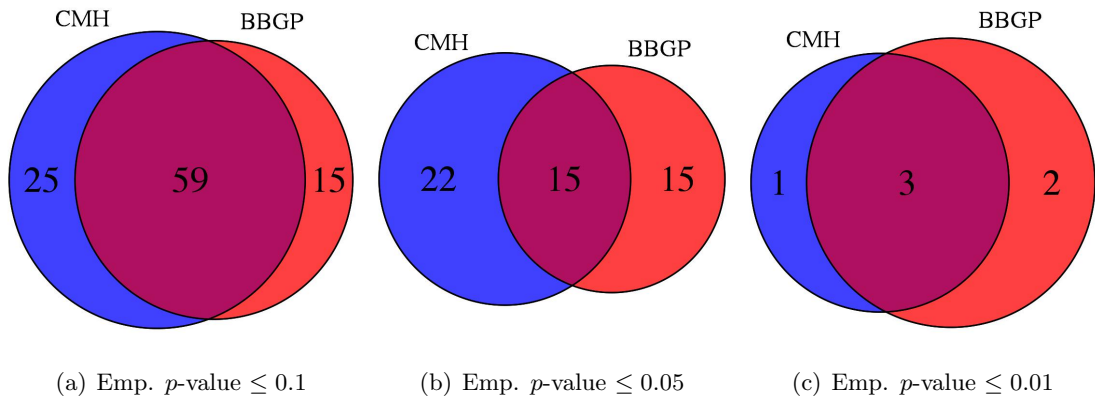


Figure 13: *Venn diagram of significantly enriched GO categories.* Empirical p -values (Emp. p -val.) for the MWU tests are calculated for each category based on sampling random SNPs (1000 times) but keeping their chromosomal order. Overlap between CMH and BBGP tests are shown for different significance levels.